Engineering bi-color emission in 2D core/crown CdSe/$CdSe_{1-x}Te_x$ nanoplatelet heterostructures by the band offset tuning

Marion Dufour[1], Violette Steinmetz[2], Eva Izquierdo[1], Thomas Pons[1], Nicolas Lequeux[1], Emmanuel Lhuillier[2], Laurent Legrand[2], Maria Chamarro[2], Thierry Barisien[2], Sandrine Ithurria[2*]

[1]Laboratoire de Physique et d'Etude des Matériaux, PSL Research University, CNRS UMR 8213, ESPCI ParisTech, 10 rue Vauquelin, 75005 Paris, France.

[2]Sorbonne Universités, UPMC Univ. Paris 06, CNRS-UMR 7588, Institut des Nanosciences de Paris, 4 place Jussieu, 75005 Paris, France

Abstract : Colloidal quantum dots (QDs) are now being used as the new generation of phosphor for displays. White light is obtained by combining the blue emission of a diode with green and red population of QDs. Having bicolor emission within a single nanocrystal population can be even more convenient. Here, we demonstrate that bicolor emission can be obtained from 2D nanoplatelets (NPLs) with a core/crown geometry. In CdSe/CdTe NPLs with type II band alignment, only the charge transfer emission was observed so far due to the very fast (<ps) transfer of the electron toward the CdSe core. Here, we show that using $CdSe_{1-x}Te_x$ alloy crown with the right composition and lateral extension reduces this charge transfer and allows the observation of dual color emission at the single particle level. One emission is coming from a recombination at the core/crown interface X_{int} and the other emission is coming from a direct recombination in the crown X_{crown}. This crown emission, non visible in pure CdSe/CdTe core crown NPLs, results from the large binding energy compared to the reduced conduction band offset existing in the alloy with intermediate (60%) Te content.

Keywords : nanoplatelets, cadmium chalcogenides, bi color emission, colloidal heterostructure, exciton transport

To whom correspondence should be sent: sandrine.ithurria@espci.fr

INTRODUCTION

Nanocrystals (NCs) have attracted a huge synthetic effort because of their tunable band gap from the UV to the THz range[1]. Their use as phosphor for display has recently become the first mass market application of these nanomaterials. In such devices, a blue GaN/InGaN diode is used to pump red and green quantum dots (QDs) instead of the Ce:YAG phosphors in order to expand the color gamut. The use of two populations of QDs is nevertheless constraining since their ratio has to be finely adjusted to take into account their different photoluminescence (PL) efficiency. In this sense, having a single NC with a double emission will be highly desirable.

Bicolor emitting NCs have already been reported.[2,3] They have been proposed as dual source for classic (ie bunched photon) and quantum light (ie antibunched photon)[4] or, to cover both visible and infrared emissions.[5] To obtain such bicolor emission two main strategies have been explored. They rely on QDs heterostructure[6,7] and on doped QDs.[8,9] In particular, the observation of a phosphorescence signal from Mn doped NCs have been extensively studied.[10] However, in most of these reports, the two PL efficiencies are very different which prevent their use as phosphor for display.

For the display application the NCs, in addition of a high PL efficiency, need to present a narrow PL signal in order to obtain a large gamut. In this sense, the 2D nanoplatelets (NPLs) are the NCs exhibiting the narrowest PL signal reported with a linewidth barely above k_bT at room temperature.[11] Since their introduction in the late 2000,[12,13] a huge synthetic effort[14] has been devoted to grow 2D heterostructures which could preserve the lack of inhomogeneous broadening[15] and the associated PL narrowness or controlled cut-off wavelength for photodetection[16,17]. Two growth approach can be studied to obtain those properties. The platelets can be grown in the thickness or[18,19], they can be grown laterally. In that case, the thickness and the confinement remain constant. With a type I CdSe/CdS band alignment, the core/crown geometry has been demonstrated to be an efficient light concentrator.[20,21] However, this is the type II CdSe/CdTe band alignment[22,23,24] which generates the largest interest because of the possibility to obtain an emission though a charge transfer state.[25] In these NPLs, the emission appears strongly redshifted with respect to the absorption of both CdSe and CdTe. This has so far been attributed to the formation of an exciton at the interface of the core and the crown where the hole stays in the CdTe crown and the electron in the CdSe core. Here, we want to use this core/crown geometry to achieve bicolor emission. Indeed, these heterostructures combine several potential advantages such as (i) a large cross section for each material which can be tuned independently from the other and (ii) three recombination paths for the exciton. It can recombine within the core, the crown or at the interface. This can, in theory, lead to up to three emission wavelengths.[26] However, the practice is much more complex, and a bicolor emission already requires a fine tuning of the recombination state and charge transfer between the different materials.

In CdSe/CdTe core/crown NPLs, only interface emission has been observed so far. This results from the fast**Erreur ! Signet non défini.** (<1ps) / immediate[27] (<100 fs) delocalization at the interface of the electrons and of the holes respectively in CdSe and in CdTe. These time ranges have to be compared with the ns photoluminescence (PL) lifetime of cadmium chalcogenide NPLs at room temperature.[28,29] Thus, recombinations in the core or in the crown are unlikely to occur. In this paper we grow CdSe/$CdSe_{1-x}Te_x$ core/crown NPLs and demonstrate that by carefully choosing the crown composition and lateral extension, a dual color emission can be obtained.

DISCUSSION

To grow CdSe/$CdSe_{1-x}Te_x$ core/crown NPLs, we first synthetize CdSe core NPLs using the procedure of the literature.[22] These NPLs have a lateral extension of 9nmx22nm and a 4 monolayers (MLs) thickness (5

planes of cadmium and 4 planes of selenium) which lead to a PL peak at 510nm. The growth of the crown is ensured by mixing Cd precursors and CdSe core NPL at high temperature (215°C) and by slowly injecting the Se and Te precursors (TOPSe and TOPTe respectively). The thickness of the NPLs is unchanged (1.3nm) while their lateral extension now reaches up to 20 nm x 100 nm, see the electron microscopy image in Figure 1c, S1 and S2. A series of NPLs with an increasing ratio of Te in the crown have been synthetized from pure CdSe up to pure CdTe with a 10% step of Te content. More details about the synthesis and characterization of the materials are given in the methods and supporting information, see Figure S1-S4 and table S1. The room temperature (RT) absorption spectra of the 11 core/crown NPLs are presented in figure 1a and show two types of optical features. First, the peaks relative to the CdSe core (510nm associated to the heavy hole exciton transition and 478 nm associated to the light hole exciton transition) can be observed for all the NPLs. A second feature resulting from the crown appears at redder wavelengths. The energy of this red peak is clearly non monotonic with the Te content. This is the signature of a bowing effect and it will be further discussed later.

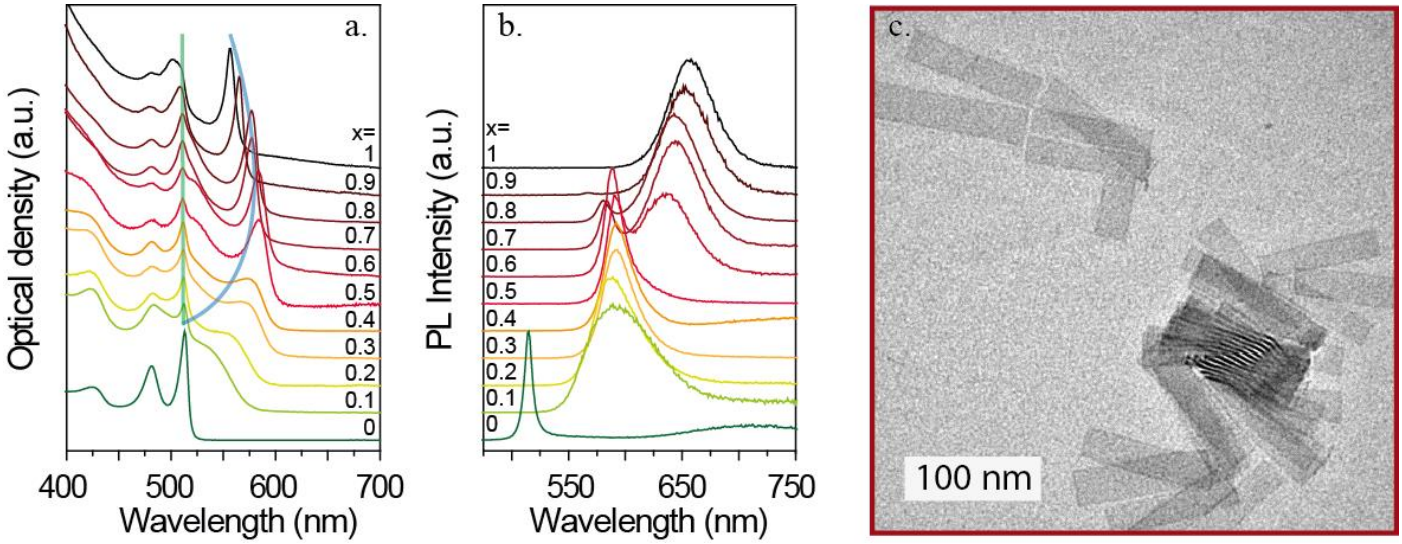

Figure 1: *(a.) RT absorption and (b.) photoluminescence spectra of solution of CdSe/CdSe$_{1-x}$Te$_x$ core/crown NPLs with $0 \leq x \leq 1$. The emission was excited at 420 nm. The absorption and luminescence background have been shifted for clarity. On figure 1(a.), the blue line (green line) corresponds to the evolution of the wavelength of the maximum of the heavy hole exciton absorption coming to the crown (core) as a function of the Te content (c.) TEM image of the CdSe/CdSe$_{0.3}$Te$_{0.7}$ core/crown NPLs*

The RT PL spectra excited at 420 nm and associated with CdSe/CdSe$_{1-x}$Te$_x$ core/crown NPLs are presented in Figure 1(b) and Figure 2. From sample to sample the spectrum drastically changes. Four main behaviors can be observed as a function of the Te content. (i) When $0<x<0.2$, we observe a single large PL peak with a typical full width half maximum (FWHM) of 160 meV, see Figure 2(c.). Previously**Erreur ! Signet non défini.**[30], it has been shown that even very little Te content leads to a significant broadening of the peak compared with pure CdSe core as well as an asymmetric shape. This is the signature of the exciton trapping due to the inhomogeneous content of the alloy.[31] (ii) For $0.3<x<0.5$, we obtain a single peak but it is narrower. The peak is also asymmetric and presents a long tail at lower energy. When x=0.5 the FWHM is equal to 19 nm, it is a typical signature of the NPLs type I emission. The peak observed in this range comes from a recombination inside the crown. The attribution of these two kinds of peaks to the alloyed crown emission is further confirmed by the fact that the PL peak is also subject to the bowing effect similar to the one observed in absorption. (iii) When $0.6<x<0.9$, the spectra present two emission peaks with very different

line widths. The high energy peak presents a limited Stokes shift with the absorption and a FWHM below 60 meV. It corresponds to the crown alloy emission. *A contrario*, the second peak at lower energy is clearly red-shifted compared to the absorption and presents a FWHM of more than 130 meV. This large peak is similar to the one observe for (iv) x=1 which has been studied and attributed to either the signature of the type II band alignment[26] or at least a recombination through interface states**Erreur ! Signet non défini.**.

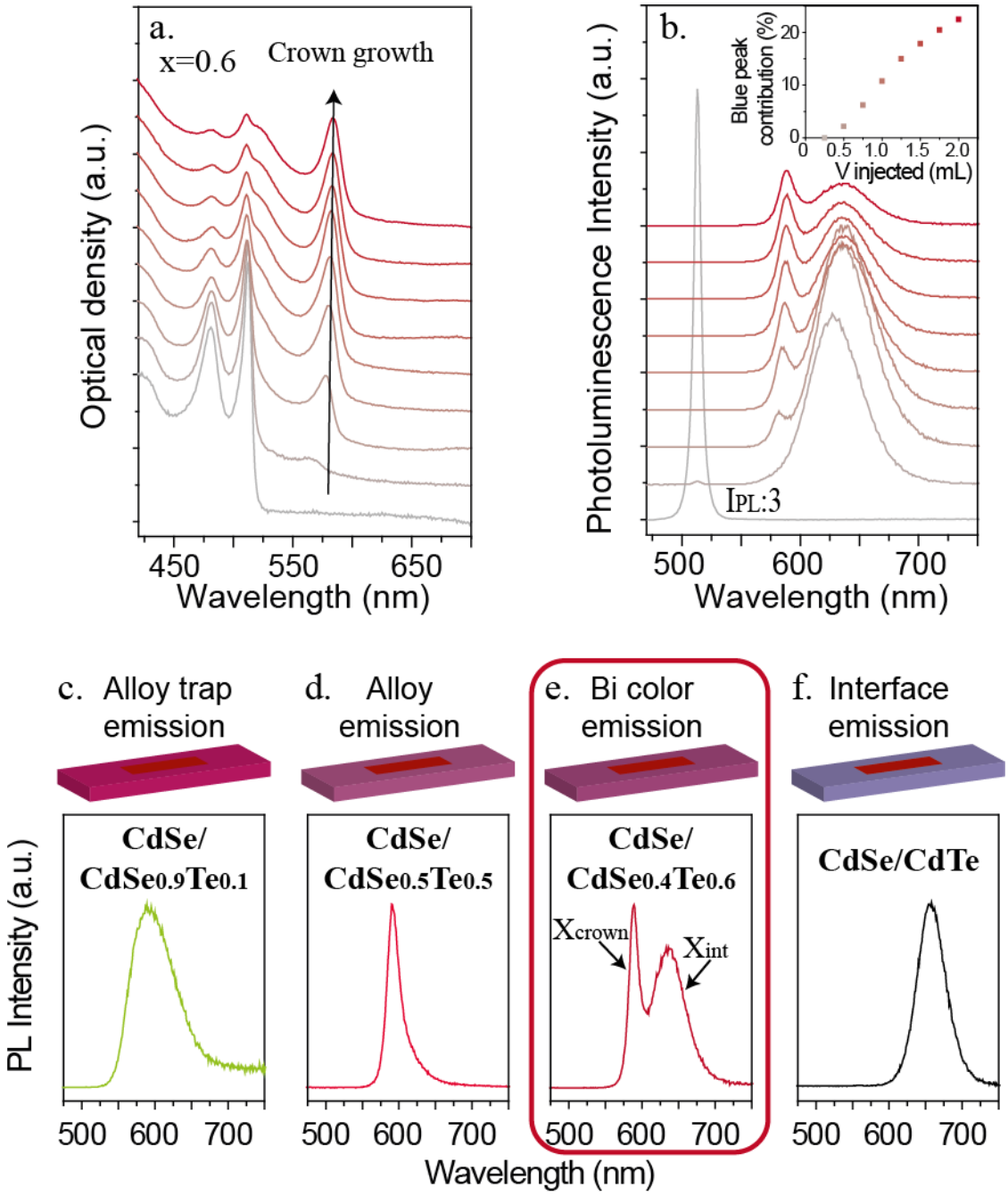

Figure 2: *(a.) RT absorption spectra of 9 aliquots taken during the synthesis of CdSe/CdSe$_{0.4}$Te$_{0.6}$ core/crown NPLs. The first grey spectrum is the NPLs before injection. Between each aliquots, the surface of the NPLs increase by about the surface of the core NPLs (see supporting information). The spectra have been normalized at 420 nm. (b.) RT photoluminescence spectra of the corresponding aliquots taken during the synthesis of CdSe/CdSe$_{0.4}$Te$_{0.6}$ core/crown. The exciton wavelength was 420 nm. The absorption and luminescence background lines have been shifted upward for clarity Inset: blue emission contribution versus injected volume. (c.), (d.), (e.) and (f.) emission and scheme of the four types of emission depending on the crown in the core/crown heterostruture.*

In the third region (iii) and, for intermediate contents of Te and Se, we observe a dual color emission made of two overlapping peaks, see Figure 2(e). These two peaks can be fitted by two Gaussian centered at 588 nm and 635 nm respectively and a full width at half maximum of 17 nm and 57 nm. We estimate that ≈25% of the signal magnitude at 588 nm (maximum of the blue peak) is actually resulting from the overlap with the red peak. To ensure that these two peaks indeed come from the same NPLs, excitation of the photoluminescence spectra centered (PLE) on the two emissions have been performed (see supporting information, figure S5) and show a perfect overlapping.

We then investigate the effect of the lateral extension of the crown on the PL emission, see Figure 2(a) and 2(b) (and supporting information figure S2 and S3). The PL peak is already strongly redshifted after the injection of 250µL of precursors. This corresponds to an increase of the NPLs surface of approximately 100%. This first large peak corresponds to the recombination through the interface. The second peak related to the crown emission only appears when the crown gets larger (typically an increase of 200% of the surface). This peak becomes more and more predominant as the crown size further increase. (inset of figure 2(b)). When we synthesize a crown with a spatial extension of only few nm the interface core/crown play an important role and the unique contribution to the emission is the interface contribution. The 2D recombination of the crown exciton becomes possible when the crown size is large enough: in NPLs, theoretical studies have indeed shown that the exciton oscillator strength is an increasing function of the lateral size before it reaches a plateau.[32] This may partly explain the progressive emergence of the crown emission with growing extension. The key role of the crown size on the relative magnitude of the two emissions is certainly the reason why Demir's group did not report about this dual color emission within CdSe/CdSe$_{1-x}$Te$_x$ core/crown NPLs. They, indeed, focused on smaller crown size and lower Te content to ensure a fine tuning of the emission from green to red with an efficient emission quantum yield.**Erreur ! Signet non défini.**

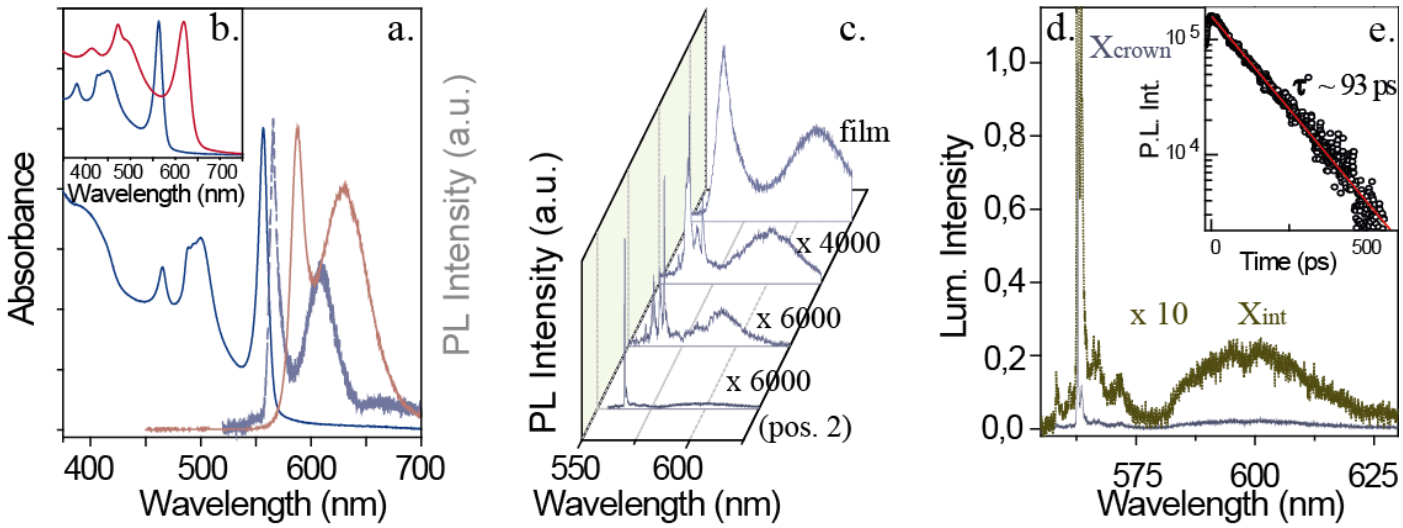

***Figure 3**: (a.) Low temperature (T~5 K) luminescence (blue-grey) and absorption (blue) of thin solid films prepared from initial solution of CdSe/CdSe$_{1-x}$Te$_x$ core/crown NPLs with x=0.6. For comparison the luminescence of NPLs in solution is also sketched (red-grey). Inset (b.): absorption of thin films for x=0.6 at ambient temperature (red) and low temperature (blue). (c.) Evolution of CdSe/CdSe$_{1-x}$Te$_x$ NPLs luminescence (x=0.6) with increasing dispersion on glass slides. The degree of dilution of used solutions (impregnation) compared to original solution is indicated above each spectrum. (d.) Typical luminescence spectrum, at ~5 K, of a single CdSe/CdSe$_{1-x}$Te$_x$ core/crown NPL (x=0.6) (dark blue). Dark green curve is a focus on the emission of the interface state (x 10). Inset (e.): Luminescence dynamics associated to the X$_{crown}$ line (562.7 nm) at ~5K and monoexponential fit of the decay (green solid line).*

In order to get insights into the intra-platelets nature of the bicolor emission, micro-PL experiments are conducted on $CdSe/CdSe_{0.4}Te_{0.6}$ NPLs for which the two PL peaks have the closest magnitude.. Spectroscopy on diluted NPLs films are carried out to ensure identification of individual optical responses. The experiments are performed at low temperature (T~5K) to reduce homogeneous broadening of the emission line that results from exciton-phonon coupling[33,34]. Figure 3(a.) compares the absorption and luminescence spectra of a low optical density film. Ambient absorption spectrums of the film as well as the luminescence of the solution are also shown. At ambient temperature, the solution and thin film have nearly identical absorption. When lowering temperature to 5 K, the film spectrum experiences a rigid blue shift (~100 meV) (see Figure 3(b.)). Such shift is expected in bulk semiconductors[35]and is primarily explained by band shifting resulting from lattice contraction and varying electron-lattice interaction. For comparison a shift of ~75 meV was measured in CdSe NPLs within the same temperature interval.[29] Slight narrowing of the absorption linewidth is also observed and is sufficient to reveal the light hole-electron (lh-e) and heavy hole-electrons (hh-e) transitions respectively from the crown and the core around 495 nm.[24] In the experiments the excitation is tuned at 515 nm (c.w. argon laser) so that only higher-lying states of the crown exciton progression get populated. In this configuration the interface state is exclusively populated from the X_{crown} exciton reservoir by exciton transfer to the core.[36] Both emission of dense films and solution present the same characteristic structure with two bands X_{int} and X_{crown}. The energy difference between the two bands (X_{crown} and X_{int}) passes from ~140 meV for NPLs in solution to 158 meV in spread NPLs at T=5 K showing that, again, temperature induced effects do not considerably modify the energy landscape of the hetero-system. Figure 3(c.) shows the evolution of low temperature PL for varying NPLs coverage rates. As the NPLs density decreases the inhomogeneous X_{crown} line splits into sharp peaks while the X_{int} emission remains identical (see Figure 3(c.)). By diluting the sample, we measure the signal from a single NPL characterized by an extremely narrow emission. Several observations evidence the intrinsic nature of the measured PL. The X_{crown} linewidths, Γ_0, are found in the range 380-450 μeV which wells compare to the values of emission widths reported in pure CdSe NPLs.[29,37] Second the emission is subject to blinking and spectral diffusion that is responsible for well resolved shifts, Δ, of the emission. In the brightest NPLs we estimate $\Delta\delta\ \Gamma_0$ within the acquisition time hence the reported Γ_0 values should be considered as upper values of the actual homogeneous widths, the latter being very likely slightly less. Measurements of the PL intensity decay for the X_{crown} line are also performed at the single NPL level. The decays are fitted using single mono-exponential functions and measurements on ~20 NPLs provide a lifetime range from 70 ps to 190 ps (a typical trace is shown in figure 3(e.)). Note that in our PL traces there is no signature of longer constants. However due to the relatively poor intensity dynamic of the detector (Streak Camera) It is not possible to exclude their presence. Our results indicate that such long time contributions, if present, have a much weaker contribution (at least one order of magnitude) at low temperature compared to the ambient situation. The measurement of sub-nanosecond decay times is a strong evidence that the X_{crown} line corresponds to the radiative recombination of a direct exciton generated in the crown. Similar decay times (~200 ps) are reported at 20K in single CdSe NPLs where the emission is only determined by the lowest band edge exciton.[29] Single object studies also directly inform about the intrinsic character of the bicolor emission. It is indeed remarkable that the interface state band X_{int} is always present in the single NPL emission as shown in figure 3(d.). The associated signal is observable in the c.w. luminescence spectrum but not in the time resolved emission (using the synchroscan camera) whereas intensity would have been expected well above the measurable threshold for sub-nanosecond decays, which confirms the long-lived nature of the state. A shared feature of single NPLs spectra is the broad spectral extension, ΔE, of the interface state emission (FWHM of ~100 meV) as well as its relative weak amplitude compared to the crown emission. We also note a more or less apparent structure in the spectrum which is found NPL dependent. In a very simple scheme, if intrinsic responses are measured, the ratio, γ, between area under the

crown line and interface state line in the single NPL spectrum should necessary roughly equals the ratio of their counterpart contributions in the inhomogeneous spectrum. This is actually verified: we find very little variations of γ within the observed NPLs and find γ~0.6-0.65 in a series of ~5 isolated NPLs exhibiting particularly well resolved emissions, directly comparable to the one extracted from the film PL following spectrum deconvolution. At low temperature single platelet emission is thus composed of a narrow exciton line similar to a QWs free exciton line, accompanied by a broad low energy band with much longer dynamics. In epitaxial double QWs, low temperature inhomogeneously broadened indirect exciton luminescence has width in the meV range[38,39], which makes a difference of nearly two orders of magnitude. One possible explanation is that the emission originates from the recombination of an electron-hole pair with one of the carriers or both in deep traps. ΔE would characterize the distribution of the energy levels associated to the traps. As investigation is at the single NPL level the following important conclusion can be drawn: the observation of narrow X_{crown} lines is a strong indication that neither hole or electron trapping due to alloy potential fluctuations, arises in the crown volume at low temperature (hence also at higher temperature).[40] As narrow free excitonic lines are also observed at low temperature in pure CdSe NPLs[29], we also come to the conclusion that trapping prevails at the interface between the core and the crown material.

In the following, we conduct time-resolved PL spectroscopy at RT to further quantify the emission dynamic and characterize the dual emission. Figure 4(a) follows the luminescence spectrum at early time (<1.5 ns) after excitation for CdSe/$CdSe_{0.4}Te_{0.6}$ core/crown NPLs. High excitation energy is used (λ=407 nm->E≈3 eV) so that both the core and the crown are excited. The density of excitation is about 4μJ/cm^{-2}. Over the first few ns, only the PL peak relative to the crown is observed while the red broad peak is extremely weak and hardly observable (see figure 4(a)). This strongly differs from the CdSe/CdTe core/crown objects for which the transfer of the electron is expected to occur over a sub ps time scale.[25,27] Time dependence of the blue peak emission at short time scale is plotted in Figure 4(b) for three samples, x=0.5 when only the crown emits, x=0.6 when both the crown and the interface emits and x=0.8 when the crown barely emits. We underline very distinct behaviors. At high Te content (x=0.8), we observe a very fast decay with a constant below the instrumental resolution (~15 ps), which already corresponds to ~30% of the integrated time resolved PL signal. When the Te content is reduced (x=0.5, 0.6) the dynamic considerably slows down and the decay can be fitted with two exponentials with characteristic times of 35 ps and 160 ps respectively. Moreover, the weight of those fast components in the total integrated time becomes much weaker, only a few percent. We then investigate the dynamics at longer time scale (>ns) for the crown emission (Figure 4(c)) and the interface emission (Figure 4(d)).[41] Decays show in general a multi-exponential dynamics that depends on x, the Te content. In particular, crown and interface emission decays are very similar for the sample CdSe/$CdSe_{0.4}Te_{0.6}$. They correspond to a multi-exponential dynamic including four components. Decay times (and respective weights) of 6 ns (0.627) , 60 ns (0.290), 250ns (0.079) and 2.0μs (0.004) are measured for the crown peak whereas the values of 18 ns (0.38), 80ns (0.44) , 350ns (0.15) and 1.7μs (0.03) characterize the interface peak dynamics. Note that the first three constants as well as their weight are determined with a rather low uncertainty (of a few percents) whereas it is higher but keeps moderate (~10%) for the last one, due to the limited extension of the observed temporal window. In a general manner the presence of a distribution of decay times may be related to exciton transport *via* hopping.[42] It thus would be tempting to ascribe the lengthening of the decays to the introduction of traps on the percolation path of excitons through alloying. However RT observation of multi-exponential dynamics with constants in the same range in the relaxation of single homo-NPLs of CdSe[29] precludes the assignment of decay lengthening to the introduction of the alloy alone. Hence the complex structure of the dynamics at longer scale will not be discussed further here. The main point of the study is the observation of a concomitant shortening of the fast component in the decay (that also gain weight) and strong decrease of the integrated X_{crown} PL with increasing x. This is clearly the indication that non radiative processes become important when the crown

composition gets closer to pure CdTe. At that point it is impossible to explicitly identify the process as corresponding to the fast electron transfer towards the core. However we emphasis that by contrast the reduced effect for intermediary compositions (x~0.6) makes favorable the populations balance towards X_{crown} compared to X_{int}.

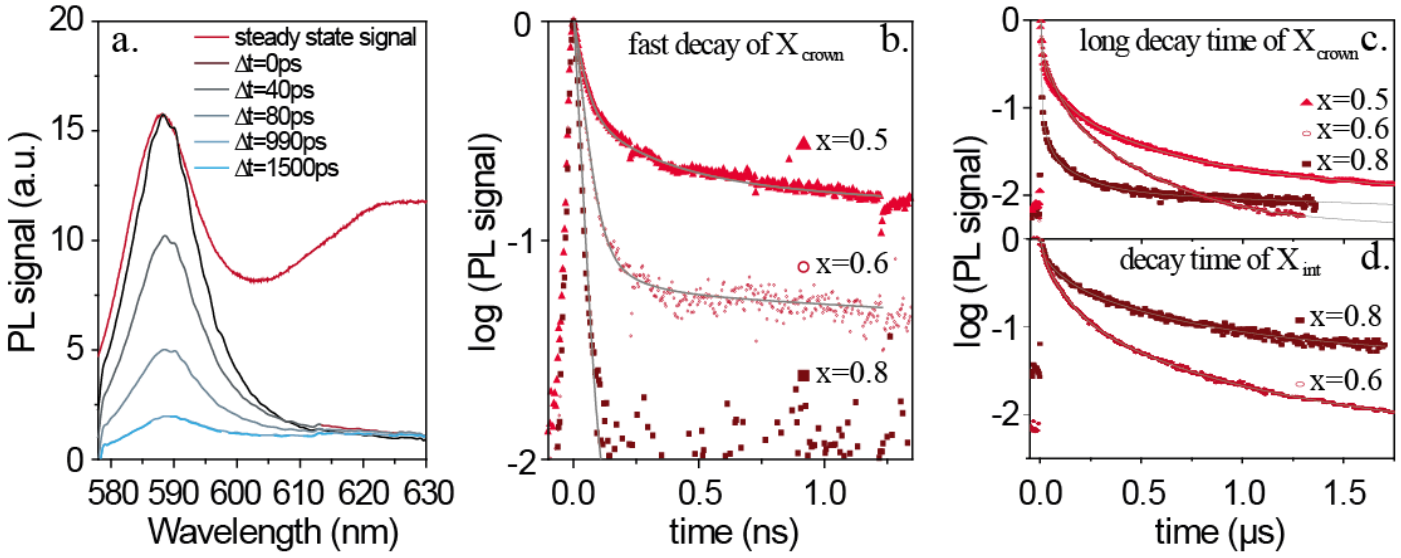

Figure 4: *(a.) PL signal for a solution of CdSe/CdSe$_{1-x}$Te$_x$ with x=0.6 at early times (t<1.5ns) after the light. For comparison, the steady signal with the two emissions peaks is plotted in dark red. (b.) PL decay at early times (t<1.5ns) for CdSe/CdSe$_{1-x}$Te$_x$ for three different x ratios of Te (x=0.5, 0.6, 0.8). A narrow band pass filtered is used to collect photon around 590nm (mainly crown emission). (c.) PL decay at long time scale for CdSe/CdSe$_{1-x}$Te$_x$ for three different x ratio of Te (x=0.5, 0.6, 0.8). The same filter as for (b.) is used. (d.) PL decay at long time scale for CdSe/CdSe$_{1-x}$Te$_x$ for two different x ratio of Te (x=0.6, 0.8) (mainly associated to the interface emission). For x=0.5, the core/crown NPLs don't exhibit emission from the interface. A narrow band pass filtered is used to collect photon around 630nm. In all cases, measurements are acquired at room temperature and the excitation wavelength is 407nm.*

We have observed a clear dependence of the PL spectra as a function of the Te content in the crown and want to further elucidate its origin. From the absorbance and PL spectra, we extract the valence (ΔV_v) and conduction (ΔV_c) band offsets between the CdSe core and the CdSe$_{1-x}$Te$_x$ crown when the dual emission happens (which means for 1<x<0.5).**Erreur ! Signet non défini.** The procedure is further detailed in the figure S6 of the supporting information. The value for ΔV_v is always large (≈0.5eV) and poorly depends on the Te content, see Figure 5(a). As a result, the holes are always promptly transferred into the crown. This explains in particular why there is no PL signature from the CdSe core. The situation is very different for the electron where ΔV_c spans from 0.15eV to 0.35eV depending on the Te content. This value has to be compared with the exciton binding energy since their relative magnitude will drive the interface charge transfer[43]. The exciton binding energy is much larger in 2D NPLs than in QDs, and is typically around 250meV.[44,45] Thus, depending on the Te content, the electron transfer driving force (ΔV_c) can be smaller or larger than the strength of the exciton Coulomb attraction (ie the exciton binding energy E_{exc}). When $\Delta V_c > E_{exc}$ which occurs at high Te content, the electron promptly gets the core/crown interface and the interface emission is only observed. On the other hand, when x is around 0.6 ($\Delta V_c < E_{exc}$) the electron remains coulombically retained in the crown. These band offsets come as a consequence of the band bowing effect occurring in alloy CdSe$_{1-x}$Te$_x$ highlighted in figure 5(a). The band gap of the crown can be fitted with the equation $E_{CdSe1-xTex}=xE_{CdTe}+(1-x)E_{CdSe}-bx(1-x)$, where b the band bowing parameter is equal to 0.78 (see figure 5(a)).

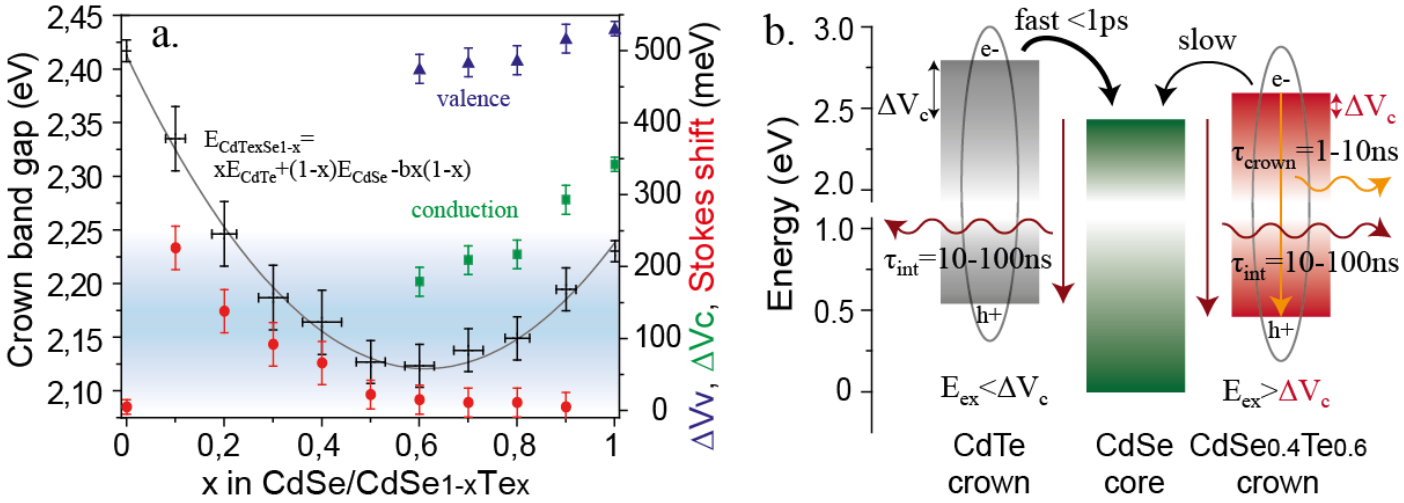

Figure : *(a.) Band gap of the $CdSe_{1-x}Te_x$ crown as a function of x between 0 and 1. The experimental points are fitted with the equation of the gap with a bowing parameter of 0.78. On the right side, the valence band ΔV_v and conduction band ΔV_c offsets between the CdSe core and the $CdSe_{1-x}Te_x$ crown and the Stokes shift between the absorption and the emission of the crown are given as a function of x. The blue zone corresponds to 250meV, a typical value of the exciton binding energy in NPLs. When the $\Delta V_c < E_{exc}$ the two emission are observable. (b.) Representation of the relative band gap of the CdSe core with respect to a CdTe and $CdSe_{0.4}Te_{0.6}$ crown.*

Thus positioning of the conduction band offset in the range of the exciton binding energy make the emission of the interface and of the crown having similar weight in the integrated time resolved luminescence and leads to the observation of bicolor emission. The evolution of the dynamics with crown composition corroborates this picture.

CONCLUSION

As a summary, we can rationalize the observation of bicolor emission by the fact that adjustment of the crown composition allows fine tuning of the conduction band offset compared to the excitonic binding energy. The latter is only made possible by the presence of bowing effect. In a consistent way short time dynamics show that when Coulomb attraction is stronger and binding states energetically more favorable, non radiative quenching of the crown exciton is also drastically reduced, very likely due to less efficient charge transfer towards the core. In addition unambiguous demonstration of the bicolor emission by individual nanoplatelets is done. This work unveils that model 2D geometries allows new possibilities at the single object level, for the design of multicolor emission compared with 0D quantum dots. Future works will be dedicated to the design of dual emitter with a larger energy splitting.

METHODS

CHEMICALS

Octadecene (ODE) (Aldrich, 90 %), Cadmium acetate dihydrate (Sigma Aldrich, 98 %), Cadmium oxide (Strem, 99.99 %), myristic acid (Aldrich, >99%), Oleic Acid (OA) (Aldrich 90 %), Trioctylphosphine (TOP) (Aldrich, 97 %), Selenium (Strem Chemicals 99.99 %), Tellurium (Aldrich, 30 mesh, 99.997 %), Hexane (Carlo Erba, 95 %), Ethanol (Carlo Erba, 99.9 %), Methanol (Carlo Erba, 99,9%)

PRECURSOR PREPARATION

TOP Se 1M

In a glove box, 50 ml of TOP are stirred with 3.95 g of selenium, overnight up to a complete dissolution of the powder.

TOP Te 1M

In a three neck flask, 2.54 g of Te powder are mixed with 20 mL of trioctylphosphine and degassed under vacuum at room temperature until the pressure gets reduced below 1 mBar. Then the flask is heated under Ar, at 275°C until the black Te powder gets fully dissolved. The orange solution is then cooled and turns yellow. Once the temperature is below 40°C, the solution is further degassed under vacuum for 10 min and finally stored in an air free glove box.

Cadmium myristate

In a 50 ml three neck flask, 1.28 g of CdO (10 mmol) and 5.5g of myristic acid (24 mmol) are degassed for 30 minutes at 70 °C. Then, under argon flow, the mixture is heated up to 200 °C for 30 minutes until it becomes colorless. At the end of the reaction 25 ml of methanol are added between 60 °C and 70 °C in order to solubilize the excess of myristic acid. The cadmium myristate is then precipitated in a centrifuge tube with addition of excess methanol. The washing procedure is repeated at least three times and the cadmium myristate is finally dried overnight under vacuum.

NANOCRSYTAL SYNTHESIS

Core CdSe 5 ML synthesis

The procedure for the synthesis of the NPLs is similar to the one described by Pedetti et al.**Erreur ! Signet non défini.** 24 mg of Se powder, 340 mg of $Cd(Myr)_2$ and 25 mL of ODE are mixed in a 50 mL three-neck flask. The solution is degassed under vacuum for 10 minutes at room temperature. Then, under an argon flow, the temperature is set to 240°C. 110 mg of $Cd(Ac)_2$ are added when the color becomes orange (200°C approximately). After 10 minutes at 240°C, the reaction is quenched with 200 µL of oleic acid and then quickly cooled to room temperature. As obtained, the solution is a mix of dots and platelets. After adding 25 mL of hexane and 25 mL of ethanol, the platelets are selectively precipitated by centrifugation at 6000 rpm for 5 minutes. The orange supernatant is removed and the precipitate is dispersed in hexane. The amount of hexane is chosen so that 100 µL of the NPLs solution diluted in 3mL of hexane have an optical density of 0.6 at 512 nm in a 1 cm cuvette.

CdSe/CdSeTe core/crown heteronanoplatelets

1.5 mL of the CdSe NPLs solution are centrifuged, the platelets are then dried and dispersed in 2 mL of ODE. In a 25 mL three-neck flask, 24 mg of $Cd(Ac)_2$, the NPLs in ODE and 45 µL of oleic acid are mixed and vacuumed at room temperature for 10 minutes. Under an argon flow the temperature is set to 215°C. In parallel, a mix a variable ratio of TOPSe (1 M) and TOPTe (1 M) in ODE is prepared (total anion concentration of 0.025 M). When the temperature is reached, this second solution is injected at a rate of 2 mL/h into the reaction media. When the desired injection volume is reached (between 0.25 mL and 2 mL), the mixture is cooled to room temperature and washed once with ethanol. The core/crown $CdSe/CdSe_xTe_{1-x}$ NPLs are suspended in hexane and stored in the dark to prevent them from photodegradation. Aliquots are taken every 0.25 ml of the second mixture injected in the three neck flask.

MATERIAL CHARACTERIZATION

UV-visible spectrum have been acquired with a Shimadzu UV-3600 spectrometer. Photomuminescence (excitation at 420 nm) and excitation spectra are obtained from an Edinburgh Instrument spectrometer.
The transmission electron microscope is a JEOL 2010. The grids are prepared by a dropcast of a solution of NPLs dispersed in hexane and degassed overnight under secondary vacuum.
X ray diffraction is conducted by dropcasting a solution of NPLs on a Si wafer. The diffractometer is a Philips X'Pert based on the emission of the Cu K_α line operated at 40 kV and 40 mA.
Energy Dispersive X ray spectroscopy (EDS) is performed using a Oxford EDS spectrometer in a FEI Magellan scanning electron microscope.

Micro-photoluminescence

Experiments are performed with a confocal-like setup using a 0.6 numerical aperture microscope objective to focus light on the nano-object and collect light in reflection configuration. Scattering light from the laser is suppressed placing a sharp edge dielectric filter from Semrock company on the collecting path. Imaging of the sample plane is made on the entrance slits plane of an imaging Acton SP2760 spectrometer (from Princeton Instruments) and luminescence detected with a nitrogen-cooled CCD camera (SPEC10 -PI). For low temperature studies core/crown NPLs are dispersed on glass slides (thickness ~100 μm) and glued on the cold finger of a micro-photoluminescence cryostat from Oxford Instrument company.

Time resolved spectroscopy

Time resolved spectroscopy was performed resorting to two distinct methods. Sub-nanosecond decays of the photoluminescence were measured using a streak-camera (C5680 model from Hamamatsu incorporating a M5675 synchroscan unit) coupled to the Acton SP2760 spectrometer. In this configuration excitation light - pulses of ~2 ps duration - is the second harmonic of a titane-sapphire laser operating at 82 MHz ; a temporal resolution of ~15 ps is then typically obtained following dispersion of the emitted light through the spectrometer. Classical gated photon counting provided access to long range decays. A gate scanning unit including a discriminator (SR400 from Stanford Research Systems) was associated to a single photon module with high efficiency in the visible spectrum (SPCM-AQRH-13-FC from Excelitas Technologies') allowing studies in the nanosecond to millisecond range with a minimal resolution of 5 ns. In this latter case a picosecond laser photodiode (from Alphalas) delivering pulses of 60 ps at λ=407 nm was used. In order to improve collection efficiency spectral selection was achieved using highly selective dichroïc filters from Semrock company. All measurement were carried out in a confocal geometry in extremely low power regimes of excitation where non linear effects were not observed.

ACKNOWLEDEGMENTS

We thank Agence Nationale de la Recherche for funding through grant Nanodose and H2DH. This work has been supported by the Region Ile-de-France in the framework of DIM Nano-K. This work was supported by French state funds managed by the ANR within the Investissements d'Avenir programme under reference ANR-11-IDEX-0004-02, and more specifically within the framework of the Cluster of Excellence MATISSE.

REFERENCES

(1) Lhuillier, E.; Scarafagio, M.; Hease, P.; Nadal, B.; Aubin, H.; Xu, X.; Lequeux, N.; Patriarche, G.; Ithurria, S.; Dubertret, B. *Nano Lett.* **2016**, acs.nanolett.5b04616.

(2) Teitelboim, A.; Meir, N.; Kazes, M.; Oron, D. *Acc. Chem. Res.* **2016**, *49* (5), 902.

(3) Brovelli, S.; Bae, W. K.; Meinardi, F.; Santiago González, B.; Lorenzon, M.; Galland, C.; Klimov, V. I. *Nano Lett.* **2014**, *14* (7), 3855.

(4) Deutsch, Z.; Schwartz, O.; Tenne, R.; Popovitz-Biro, R.; Oron, D. *Nano Lett.* **2012**, *12* (6), 2948.

(5) Lin, Q.; Makarov, N. S.; Koh, W. K.; Velizhanin, K. a.; Cirloganu, C. M.; Luo, H.; Klimov, V. I.; Pietryga, J. M. *ACS Nano* **2015**, *9* (1), 539.

(6) Pinchetti, V.; Meinardi, F.; Camellini, A.; Sirigu, G.; Christodoulou, S.; Bae, W. K.; De Donato, F.; Manna, L.; Zavelani-Rossi, M.; Moreels, I.; Klimov, V. I.; Brovelli, S. *ACS Nano* **2016**, *10* (7), 6877.

(7) Soni, U.; Pal, A.; Singh, S.; Mittal, M.; Yadav, S.; Elangovan, R.; Sapra, S. *ACS Nano* **2014**, *8* (1), 113.

(8) Vlaskin, V. A.; Janssen, N.; Van Rijssel, J.; Beaulac, R.; Gamelin, D. R. *Nano Lett.* **2010**, *10* (9), 3670.

(9) Jo, D. Y.; Kim, D.; Kim, J. H.; Chae, H.; Seo, H. J.; Do, Y. R.; Yang, H. *ACS Appl. Mater. Interfaces* **2016**, *8* (19), 12291.

(10) Panda, S. K.; Hickey, S. G.; Demir, H. V.; Eychmüller, A. *Angew. Chemie - Int. Ed.* **2011**, *50* (19), 4432.

(11) Pedetti, S.; Nadal, B.; Lhuillier, E.; Mahler, B.; Bouet, C.; Abécassis, B.; Xu, X.; Dubertret, B. *Chem. Mater.* **2013**, *25* (12), 2455.

(12) Joo, J.; Son, J. S.; Kwon, S. G.; Yu, J. H.; Hyeon, T. *J. Am. Chem. Soc.* **2006**, *128* (17), 5632.

(13) Ithurria, S.; Dubertret, B. *J. Am. Chem. Soc.* **2008**, *130* (49), 16504.

(14) Nasilowski, M.; Mahler, B.; Lhuillier, E.; Ithurria, S.; Dubertret, B. *Chem. Rev.* **2016**, *116* (18), 10934.

(15) Lhuillier, E.; Pedetti, S.; Ithurria, S.; Nadal, B.; Heuclin, H.; Dubertret, B. *Acc. Chem. Res.* **2015**, *48* (1), 22.

(16) Lhuillier, E.; Dayen, J. F.; Thomas, D. O.; Robin, A.; Doudin, B.; Dubertret, B. *Nano Lett.* **2015**, *15* (3), 1736.

(17) Lhuillier, E.; Robin, A.; Ithurria, S.; Aubin, H.; Dubertret, B. *Nano Lett.* **2014**, *14* (5), 2715.

(18) Ithurria, S.; Talapin, D. V. *J. Am. Chem. Soc.* **2012**, *134* (45), 18585.

(19) Mahler, B.; Nadal, B.; Bouet, C.; Patriarche, G.; Dubertret, B. *J. Am. Chem. Soc.* **2012**, *134* (45), 18591.

(20) Prudnikau, A.; Chuvilin, A.; Artemyev, M. *J. Am. Chem. Soc.* **2013**, *135* (39), 14476.

(21) Tessier, M. D.; Spinicelli, P.; Dupont, D.; Patriarche, G.; Ithurria, S.; Dubertret, B. *Nano Lett.* **2014**, *14* (1), 207.

(22) Antanovich, a. V.; Prudnikau, a. V.; Melnikau, D.; Rakovich, Y. P.; Chuvilin, A.; Woggon, U.; Achtstein, A. W.; Artemyev, M. V. *Nanoscale* **2015**, *7* (17), 8084.

(23) Kelestemur, Y.; Olutas, M.; Delikanli, S.; Guzelturk, B.; Akgul, M. Z.; Demir, H. V. *J. Phys. Chem. C* **2015**, *119* (4), 2177.

(24) Pedetti, S.; Ithurria, S.; Heuclin, H.; Patriarche, G.; Dubertret, B. *J. Am. Chem. Soc.* **2014**, *136* (46), 16430.

(25) Li, Q.; Zhou, B.; McBride, J. R.; Lian, T. *ACS Energy Lett.* **2016**, acsenergylett.6b00634.

(26) Li, Q.; Xu, Z.; McBride, J. R.; Lian, T. *ACS Nano* **2017**, acsnano.6b08674.

(27) Cassette, E.; Pedetti, S.; Mahler, B.; Ithurria, S.; Dubertret, B.; Scholes, G. *Phys. Chem. Chem. Phys.* **2017**, *19*, 8373.

(28) Ithurria, S.; Tessier, M. D.; Mahler, B.; Lobo, R. P. S. M.; Dubertret, B.; Efros, A. L. *Nature Materials*. 2011, pp 936–941.

(29) Tessier, M. D.; Javaux, C.; Maksimovic, I.; Loriette, V.; Dubertret, B. *ACS Nano* **2012**, *6* (8), 6751.

(30) Kelestemur, Y.; Guzelturk, B.; Erdem, O.; Olutas, M.; Erdem, T.; Usanmaz, C. F.; Gungor, K.; Demir, H. V. *J. Phys. Chem. C* **2017**, acs.jpcc.6b11809.

(31) Tenne, R.; Pedetti, S.; Kazes, M.; Ithurria, S.; Houben, L.; Nadal, B.; Oron, D.; Dubertret, B. *Phys. Chem. Chem. Phys.* **2016**, *18* (22), 15295.

(32) Bose, S.; Song, Z.; Fan, W. J.; Zhang, D. H. *J. Appl. Phys.* **2016**, *119* (14).

(33) Cui, J.; Beyler, A. P.; Coropceanu, I.; Cleary, L.; Avila, T. R.; Chen, Y.; Cordero, J. M.; Heathcote, S. L.; Harris, D. K.; Chen, O.; Cao, J.; Bawendi, M. G. *Nano Lett.* **2016**, *16* (1), 289.

(34) Takagahara, T. *Phys. Rev.* **1993**, *70* (10), 1553.

(35) Varshni, Y. P. *Physica* **1967**, *34* (1), 149.

(36) Wu, K.; Li, Q.; Jia, Y.; McBride, J. R.; Xie, Z. X.; Lian, T. *ACS Nano* **2015**, *9* (1), 961.

(37) Citrin, D. S. *Phys. Rev. B* **1993**, *47* (7), 3832.

(38) Krivolapchuk, V. V.; Moskalenko, E. S.; Zhmodikov, a. L. *Phys. Rev. B* **2001**, *64* (4), 045313.

(39) Butov, L. V.; Filin, a. I. *Phys. Rev. B* **1998**, *58* (4), 1980.

(40) Schwab, H.; Dörnfeld, C.; Göbel, E. O.; Hvam, J. M.; Klingshirn, C.; Kuhl, J.; Lyssenko, V. G.; Majumder, F. a.; Noll, G.; Nunnenkamp, J.; Pantke, K. H.; Renner, R.; Reznitsky, A.; Siegner, U.; Swoboda, H. E.; Weber, C. *Phys. Status Solidi* **1992**, *172* (2), 479.

(41) Scott, R.; Kickhöfel, S.; Schoeps, O.; Antanovich, A.; Prudnikau, A.; Chuvilin, A.; Woggon, U.; Artemyev, M.; Achtstein, A. W. *Phys. Chem. Chem. Phys.* **2016**, *18* (4), 3197.

(42) Sturman, B.; Podivilov, E.; Gorkunov, M. *Phys. Rev. Lett.* **2003**, *91* (October), 176602.

(43) Robin, A.; Lhuillier, E.; Xu, X. Z.; Ithurria, S.; Aubin, H.; Ouerghi, A.; Dubertret, B. *Sci. Rep.* **2016**, *6*, 24909.

(44) Benchamekh, R.; Gippius, N. A.; Even, J.; Nestoklon, M. O.; Jancu, J. M.; Ithurria, S.; Dubertret, B.; Efros, A. L.; Voisin, P. *Phys. Rev. B - Condens. Matter Mater. Phys.* **2014**, *89* (3).

(45) Achtstein, A. W.; Schliwa, A.; Prudnikau, A.; Hardzei, M.; Artemyev, M. V; Thomsen, C.; Woggon, U. **2012**.

Table of Contents: